

The DCN/HCN abundance ratio in hot molecular cores

J. Hatchell, T.J. Millar, and S.D. Rodgers

Department of Physics, UMIST, P.O. Box 88, Manchester M60 1QD, UK

Received 13 November 1997 / Accepted 5 January 1998

Abstract. We have observed the 3-2 transitions of DCN and HC^{15}N in a number of hot molecular cores previously surveyed by us with the interesting result that the DCN/HCN ratio is low, a few times 10^{-3} , in the hot cores. The abundance ratio of DCN/HCN is derived both ‘on-core’ and ‘off-core’ and, in general is larger at the ‘off-core’ positions. Comparison with chemical models of these sources indicates that DCN liberated from evaporated ices can be destroyed rapidly in the hot gas by reaction with atomic hydrogen, which works to reset the the initial DCN/HCN ratio in the ice to the gas-phase atomic D/H ratio. The low DCN/HCN abundance ratio we measure can be reached in less than 10^4 years, consistent with previous estimates of the core ages, if the activation energy of the reaction is less than 500 K.

Key words: ISM: abundances – ISM: molecules – radio lines: ISM – molecular processes

1. Introduction

The enhancement of deuterium observed in several species, including HDO, NH_2D , HDCO and CH_3OD , is strong evidence that the gas-phase composition of hot molecular cores reflects, to a certain extent, a previous cold phase in the molecular evolution of the gas since such fractionation, dependent as it is on small zero-point energy differences, can occur effectively only at very low temperatures. At present, there is a debate as to whether the chemistry in the cold phase is dominated by surface or gas-phase reactions. Brown & Millar (1989a,b) explored the possibility that grain surface reactions are active in the hydrogenation and deuteration of atoms and radicals through the addition of H and D atoms, arguing that only such an additional mechanism could account for the larger fractional abundance of NH_2D detected in hot cores compared to cold, dark clouds. In their model, and those of Charnley, Tielens & Millar (1992) and Caselli, Hasagawa & Herbst (1993), the evaporation of small, saturated molecules from ice mantles in hot cores drives the formation of more complex organic molecules in the

hot gas. However, recent single-dish observations of ethanol (Millar, Macdonald & Habing 1995, Ohishi et al. 1995) and other complex molecules (Macdonald et al. 1996, Hatchell et al. 1998), as well as interferometer observations (Miao et al. 1995, Kuan, Mehringer & Snyder 1996, Mehringer & Snyder 1996, Miao & Snyder 1997) indicate that the molecular abundances of these species relative to H_2 are $\sim 10^{-9} - 10^{-7}$, more typical of abundances of simple molecules in cold clouds, and often several orders of magnitude larger than can be produced in the most comprehensive chemical gas-phase-only models (Millar, Macdonald & Gibb 1997). The conclusion is that grain surface reactions must produce complex as well as simple molecules.

Although this general conclusion is fairly firm, the details of the surface chemistry remain unclear. Since the degree of deuterium fractionation depends on the detailed production routes to particular species (Brown & Rice 1986, Millar, Bennett & Herbst 1989, Turner 1989, Howe & Millar 1993), it is of interest to study the abundances of D-bearing molecules in hot molecular cores. Rodgers & Millar (1996) have shown that the degree of deuterium fractionation present in the ice mantles survives for a period $\sim 10^4$ yrs after evaporation so that observations of deuterated species in the gas leads directly, in most cases, to the fractionation ratio in the ice. Charnley, Tielens & Rodgers (1997) have used this approach to infer the detailed probabilities for the addition of H and D atoms to CO to form HDCO, D_2CO , CH_3OD and CH_2DOH , all of which are observed in the Orion Compact Ridge.

For these reasons, we have begun a programme to study D-bearing species in a number of hot cores in which we have also performed a molecular line survey (Hatchell et al. 1998) and in this paper report our results for the DCN/HCN ratio. Sect. 2 discusses the observations and Sect. 3 the implications for chemistry in hot molecular cores.

2. Observations and analysis

In order to derive an accurate abundance ratio it is necessary to choose optically thin lines with comparable excitation conditions. For this reason, we choose to observe the 3-2 transitions of DCN at 217.24 GHz and HC^{15}N at 258.16 GHz. Observations

Table 1. Positions, distances and molecular hydrogen column density (from Hatchell et al. 1998) for observed objects

| Object | α_{1950} [h m s] | δ_{1950} [° ' "] | d kpc | N_{H_2} 10^{24} cm^{-2} |
|-------------|------------------------------|------------------------------|------------|---|
| G5.89–0.39 | 17 57 26.8 | –24 03 56 | 2.5 | 0.6 |
| G9.62+0.19 | 18 03 16.2 | –20 32 03 | 5.7 | 1.2 |
| G10.47+0.03 | 18 05 40.3 | –19 52 21 | 5.8 | 0.9 |
| G12.21–0.10 | 18 09 43.7 | –18 25 09 | 13.5 | 4.8 |
| G29.96–0.02 | 18 43 27.1 | –02 42 36 | 7.4 | 0.7 |
| G31.41+0.31 | 18 44 59.4 | –01 16 04 | 7.9 | 0.7 |
| G34.26+0.15 | 18 50 46.1 | 01 11 12 | 4.0 | 3.6 |
| G45.47+0.05 | 19 12 04.4 | 11 04 11 | 6.0 | 0.1 |
| G75.78+0.34 | 20 19 52.0 | 37 17 02 | 4.1 | 1.1 |

were made at the James Clerk Maxwell Telescope (JCMT)¹ in May 1997 using receiver A2 (230 GHz band). Typical system temperatures were 400–700 K. The signal was analysed over a 760 MHz bandwidth using the Dutch Autocorrelation Spectrometer and all data were calibrated by the usual chopper wheel method and corrected for forward spillover and scattering to give T_{R}^* . The half-power beamwidth varies from 21'' at 217 GHz to 18'' at 258 GHz. Pointing was checked regularly and errors found to be less than 3''.

Since receiver A2 is a double sideband instrument (with sidebands separated by 3 GHz), we assigned lines to upper and lower sidebands by either shifting the central frequency by 10 MHz, which causes lines in the two sidebands to move by this amount in opposite directions, or, more commonly, by placing the observed lines first in the USB and then in the LSB. This ensures that the image band is different in both cases and allows secure identifications to be made as well as covering an additional 760 MHz in frequency.

Table 1 lists the sources observed together with their ‘on-core’ positions which denote the peaks of the hot molecular gas. We have also observed both lines toward ‘off-core’ positions, all at an offset (0,20'') from the ‘on-core’ positions. Our molecular line survey of these hot cores has shown that the ‘off-core’ positions have much less molecular emission than ‘on-core’ indicating that the hot cores are centrally condensed (Hatchell et al. 1998). Hatchell et al. found that all the line-rich sources were fit by a ‘core-halo’ structure in which a very hot and dense ($T \sim 100$ K, $n \sim 10^8 \text{ cm}^{-3}$, typically) core is surrounded by a warm and less dense ($T \sim 30$ K, $n \sim 10^5 \text{ cm}^{-3}$) halo, whilst the line-poor sources are consistent with the presence of the halo gas only. Our observations ‘on-core’ and ‘off-core’ thus allow us to separate out core and halo contributions.

¹ The JCMT is operated by the Joint Astronomy Centre on behalf of the Particle Physics and Astronomy Research Council of the United Kingdom, the Netherlands Organisation for Scientific Research, and the National Research Council of Canada.

Table 2. Observed line intensities in DCN and HC¹⁵N. Where the line intensity was less than 3σ , the 3σ upper limit is given.

| Source | $T_{\text{R}}^* \Delta v / \text{K km s}^{-1}$ | |
|-------------|--|--------------------|
| | DCN | HC ¹⁵ N |
| G5.89 (on) | 8.7 ± 0.2 | 11.8 ± 0.5 |
| (off) | < 0.6 | < 1.5 |
| G9.62 (on) | 3.6 ± 0.3 | 5.2 ± 0.4 |
| (off) | 2.5 ± 0.2 | < 2.1 |
| G10.47 (on) | 10.6 ± 0.5 | 6.1 ± 1.1 |
| (off) | 1.8 ± 0.2 | < 1.4 |
| G12.21 (on) | 2.4 ± 0.3 | < 1.2 |
| (off) | < 0.8 | < 1.7 |
| G29.96 (on) | 3.9 ± 0.2 | 4.6 ± 0.5 |
| (off) | < 0.5 | < 1.7 |
| G31.41 (on) | 5.3 ± 0.4 | 8.0 ± 0.8 |
| (off) | < 0.6 | < 1.6 |
| G34.26 (on) | 10.9 ± 0.4 | 22.8 ± 1.4 |
| (off) | 3.5 ± 0.4 | < 2.3 |
| G45.47 (on) | < 0.5 | < 1.3 |
| (off) | < 0.7 | < 1.3 |
| G75.78 (on) | 3.0 ± 0.2 | < 0.8 |
| (off) | < 0.7 | < 1.1 |

Spectra of the DCN and HC¹⁵N transitions are given in Figs. 1 and 2 respectively. Table 2 presents our results for $T_{\text{R}}^* \Delta v$, from Gaussian fits to the lines. Upper limits are 3σ . The DCN is blended with HCOOCH₃ in the lower sideband, so we use only $T_{\text{R}}^* \Delta v$ of the unblended upper sideband line. HC¹⁵N is blended with a ¹³CH₃OH line at 255.265 GHz in the upper sideband. The lower sideband spectra cannot be used instead as they were only observed for three sources. From comparison with the 255.120 GHz ¹³CH₃OH line, which we predict to have similar or greater T_{R}^* than the 255.265 GHz blending line for temperatures between 20 and 100 K, we estimate the maximum contribution of ¹³CH₃OH to the HC¹⁵N $T_{\text{R}}^* \Delta v$ to be 65% in G10.47, 20% in G29.96, G31.41 and G34.26 and less than the uncertainty due to noise in the other sources. The lower sideband spectra confirm that the ¹³CH₃OH contribution is small in G9.62, G29.96 and G75.78. In G5.89, which was observed with a slightly different centre frequency, the HC¹⁵N line is blended with CH₃OH rather than ¹³CH₃OH. We estimate the contribution of the CH₃OH line to be less than 50%, from measurements of other CH₃OH lines in G5.89. In G10.47, the surrogate ¹³CH₃OH line is sufficiently strong to get a reliable measure of $T_{\text{R}}^* \Delta v = 10.9$, and we have subtracted the ¹³CH₃OH contribution to the HC¹⁵N $T_{\text{R}}^* \Delta v$. For the other sources, where the ¹³CH₃OH contribution is $< 20\%$, and for G5.89, where there is no suitable surrogate line, we were unable to estimate $T_{\text{R}}^* \Delta v$ accurately for the blending line and have not made the correction. The resulting uncertainties in the DCN/HCN ratio are of similar order to those resulting from the uncertainty in the [¹⁴N]/[¹⁵N] ratio (see below).

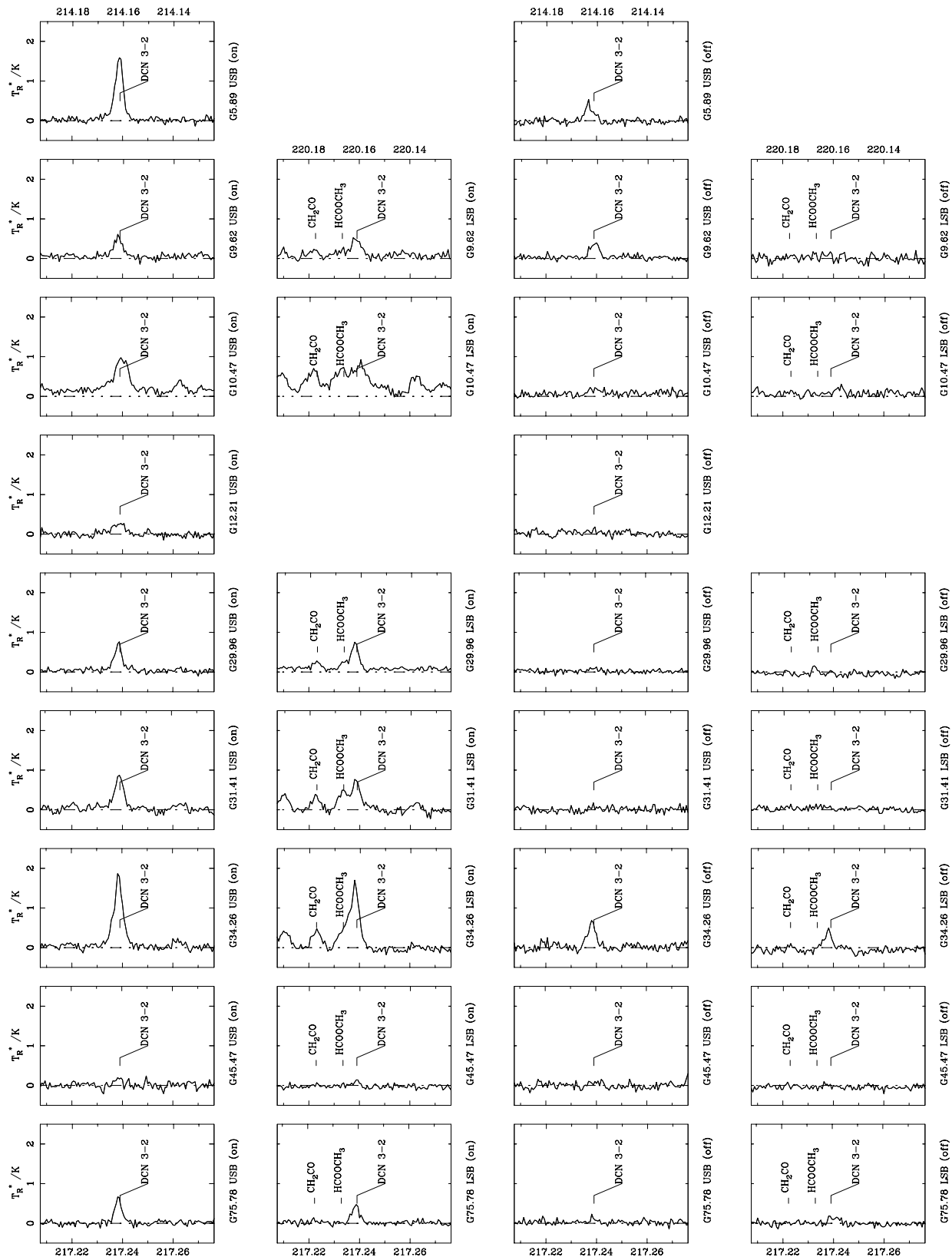


Fig. 1. Spectra of the DCN 217.24 GHz line as observed in upper sideband (USB) and lower sideband (LSB) both on and off source (offsets (0,0) and (0,20'') respectively). Columns are (left to right): On-source, upper sideband; on-source, lower sideband; off source, upper sideband; and off source, lower sideband. The lower frequency scales are for the main sideband and the upper scales give the upper and lower sideband counterparts.

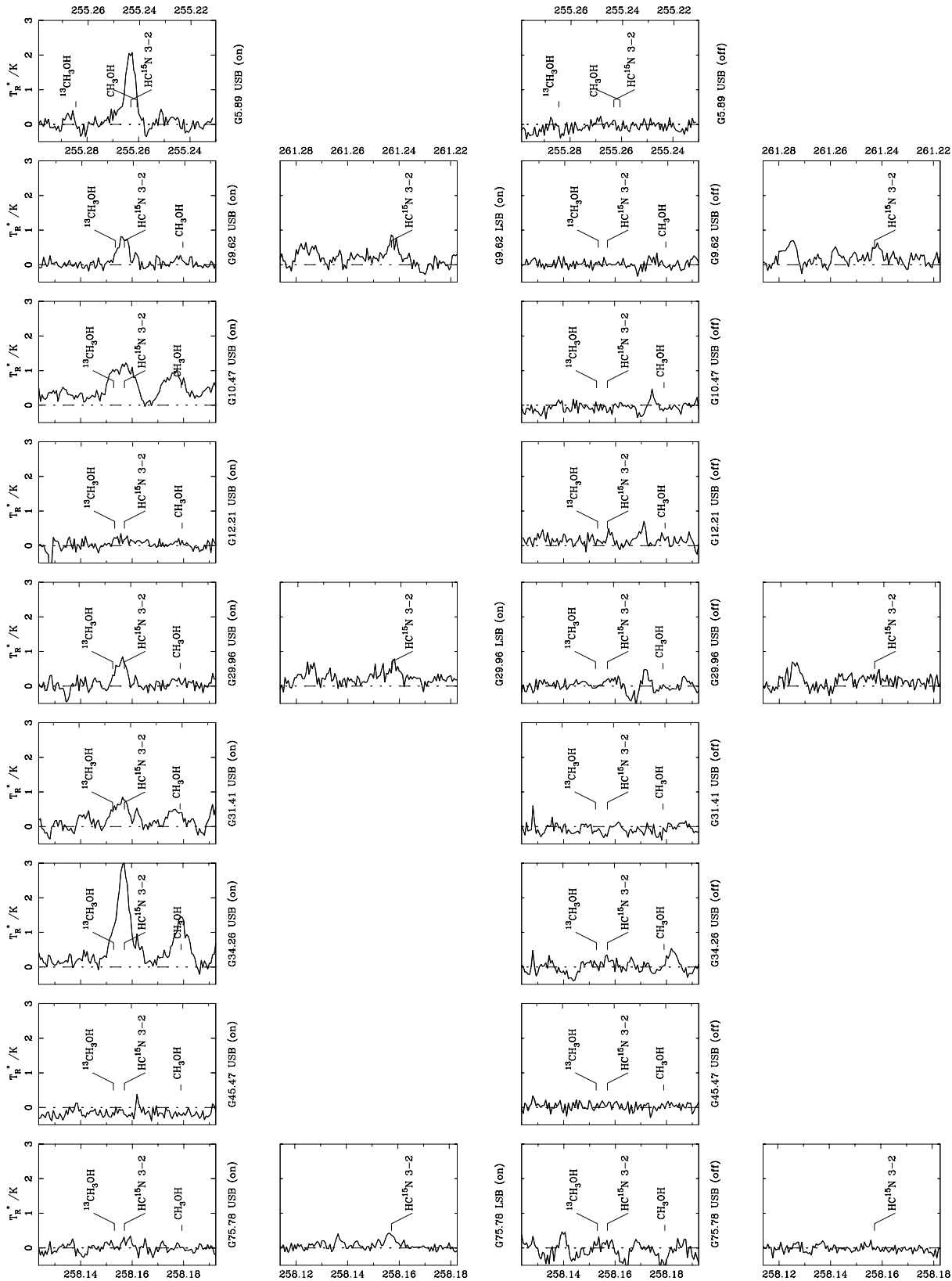


Fig. 2. Spectra of the HC^{15}N 258.16 GHz line as observed in upper sideband (USB) and lower sideband (LSB) both on and off source (offsets (0,0) and (0,20'') respectively). Columns are (left to right): On-source, upper sideband; on-source, lower sideband; off source, upper sideband; and off source, lower sideband. The lower frequency scales are for the main sideband and the upper scales give the upper and lower sideband counterparts. Note that the USB frequency scales for G5.89 are shifted with respect to those for the other sources.

We assume the lines are optically thin and extended relative to the beam (see below), and that excitation temperatures are equal in both species. The abundance ratios can then be written as:

$$\frac{N(\text{DCN})}{N(\text{HC}^{15}\text{N})} = \frac{I_{\text{D}} Q_{\text{D}}(T_{\text{x}}) \nu_{\text{H}}}{I_{\text{H}} Q_{\text{H}}(T_{\text{x}}) \nu_{\text{D}}} e^{(E_{\text{D}} - E_{\text{H}})/kT_{\text{x}}}$$

where the subscripts ‘D’ and ‘H’ refer to DCN and HC^{15}N , respectively, I is the integrated line intensity (K km s^{-1}), ν the observed line frequency, $Q(T_{\text{x}})$ the partition function at an excitation temperature, T_{x} , and E is the energy of the $J = 3$ level. In the limit that $hB < kT_{\text{x}}$, the partition function can be written as

$$Q(T_{\text{x}}) = \frac{kT_{\text{x}}}{hB}$$

where B is the rotational constant of the molecule, and since $B \propto \nu$, the abundance ratio becomes

$$\frac{N(\text{DCN})}{N(\text{HC}^{15}\text{N})} = \frac{I_{\text{D}}}{I_{\text{H}}} \left(\frac{\nu_{\text{H}}}{\nu_{\text{D}}}\right)^2 e^{(E_{\text{D}} - E_{\text{H}})/kT_{\text{x}}}$$

Using $E_{\text{D}}/k = 24.79 \text{ K}$ and $E_{\text{H}}/k = 20.86 \text{ K}$, we find that

$$\frac{N(\text{DCN})}{N(\text{HCN})} = \frac{[^{15}\text{N}]}{[^{14}\text{N}]} \frac{I_{\text{D}}}{I_{\text{H}}} \left(\frac{\nu_{\text{H}}}{\nu_{\text{D}}}\right)^2 e^{3.93/T_{\text{x}}}$$

For the isotopic ratio $[^{14}\text{N}]/[^{15}\text{N}]$, we take a constant value of 400. Studies of the nitrogen isotope abundance outside the Galactic Centre prefer a slight gradient with galactocentric radius but with large uncertainties on the parameters (Dahmen et al. 1995). A value of 400 is within 20% of the best fit values for our source galactocentric distances of between 3 and 9 kpc. This uncertainty is the main source of uncertainty in the DCN/HCN abundance ratios.

If the sources are extended relative to the beam, as appears to be the case (see below), the abundance ratio is altered by the ratio of the beam sizes, a factor of $(\nu_{\text{H}}/\nu_{\text{D}})^{-2}$, so that finally we have

$$\frac{N(\text{DCN})}{N(\text{HCN})} = \frac{[^{15}\text{N}]}{[^{14}\text{N}]} \frac{I_{\text{D}}}{I_{\text{H}}} e^{3.93/T_{\text{x}}}$$

This ratio is given in Table 3 for a range of excitation temperatures although it is only weakly dependent on T_{x} since $|E_{\text{D}} - E_{\text{H}}|/k$ is small compared to T_{x} . Our observations of only one transition do not allow us to determine T_{x} but A. G. Gibb (private communication) has observed the HC^{15}N 4–3 transition in G34.26 and estimates T_{x} to be 55 K on-core, decreasing to ~ 10 –20 K at an offset of $15''$.

Beam-averaged column densities are given in Tables 4 and 5. These are more sensitive to temperature. Assuming an extended source and comparing with values for N_{H_2} of order 10^{24} cm^{-2} (Table 1; Hatchell et al. 1998), we see that DCN and HC^{15}N abundances are a few times 10^{-11} , comparable to the Orion Extended Ridge (Blake et al. 1987).

Despite having chosen rarer isotopes of HCN, it is possible given sufficient density to have high optical depths in these transitions. If the emission regions are extended, this is unlikely to be the case. Total molecular column densities in these cores

Table 3. DCN/HCN ratios and lower limits calculated for a range of excitation temperatures. A dash indicates that both the DCN and HC^{15}N line intensities were less than 3σ . The uncertainties quoted are from spectral noise and do not include $\sim 20\%$ for uncertainties in $[^{14}\text{N}]/[^{15}\text{N}]$, or uncertainties due to blending of HC^{15}N with $^{13}\text{CH}_3\text{OH}$, except in the case of G10.47.

| Source | [DCN]/[HCN] $\times 10^{-4}$ | | | |
|--------------|------------------------------|----------------|----------------|----------------|
| | $T_{\text{x}} = 20$ | 30 | 50 | 100 K |
| G5.89 (on) | 14.4 \pm 0.7 | 15.6 \pm 0.8 | 16.7 \pm 0.8 | 17.5 \pm 0.9 |
| G5.89 (off) | – | – | – | – |
| G9.62 (on) | 13.6 \pm 1.3 | 14.8 \pm 1.4 | 15.8 \pm 1.5 | 16.6 \pm 1.6 |
| G9.62 (off) | > 35.4 | > 38.5 | > 41.1 | > 43.3 |
| G10.47 (on) | 33.7 \pm 6.5 | 36.7 \pm 7.1 | 39.2 \pm 7.6 | 41.2 \pm 8.0 |
| G10.47 (off) | > 25.3 | > 27.5 | > 29.4 | > 30.9 |
| G12.21 (on) | > 35.9 | > 39.0 | > 41.7 | > 43.9 |
| G12.21 (off) | – | – | – | – |
| G29.96 (on) | 16.8 \pm 1.8 | 18.2 \pm 2.0 | 19.5 \pm 2.1 | 20.5 \pm 2.2 |
| G29.96 (off) | – | – | – | – |
| G31.41 (on) | 13.0 \pm 1.5 | 14.1 \pm 1.6 | 15.1 \pm 1.7 | 15.8 \pm 1.8 |
| G31.41 (off) | – | – | – | – |
| G34.26 (on) | 9.3 \pm 0.6 | 10.1 \pm 0.7 | 10.8 \pm 0.7 | 11.4 \pm 0.8 |
| G34.26 (off) | > 30.0 | > 32.6 | > 34.8 | > 36.6 |
| G45.47 (on) | – | – | – | – |
| G45.47 (off) | – | – | – | – |
| G75.78 (on) | > 45.9 | > 49.9 | > 53.3 | > 56.1 |
| G75.78 (off) | – | – | – | – |

are very high ($\sim 10^{24} \text{ cm}^{-2}$, Hatchell et al. 1998). However, line intensities of $< 2 \text{ K}$ (Figs. 1, 2) imply either optically thin emission or a small source size if the lines are optically thick. The column densities required for $\tau \gtrsim 1$ in DCN or HC^{15}N are of order of 10^{15} cm^{-2} at 50 K, compared to measured beam-averaged column densities of order 10^{13} cm^{-2} . DCN is observed at many of the off positions, and this points towards an extended, optically thin source. The off-source positions are a beamwidth away from the on-source, and the emission observed could not be produced by a compact central source. A map of G34.26 in HC^{15}N also indicates an extended source (Gibb, private communication).

3. Discussion

The ‘on-core’ abundance ratios derived, $(0.9 - 4.1)10^{-3}$, for DCN/HCN are remarkably constant from source to source and are an order of magnitude smaller than those derived in TMC-1 (0.023 ± 0.001 , Wootten 1987) and the Orion Ridge Cloud (0.04 ± 0.01 , Schilke et al. 1992), the chemistries of which are dominated by gas-phase reactions, but are similar to those in the Orion Hot Core, where DCN/HCN = 0.003 (Schilke et al. 1992). Our ‘off-core’ ratios are larger since we have detected DCN, but not HC^{15}N in some positions. This behaviour is also consistent with that in Orion, and could be due to a number of effects.

Table 4. DCN column densities and 3σ upper limits calculated for a range of excitation temperatures.

| Source | N(DCN) $\times 10^{12}$ cm $^{-2}$ | | | |
|--------------|------------------------------------|----------------|----------------|----------------|
| | $T_x = 20$ | 30 | 50 | 100 K |
| G5.89 (on) | 7.9 \pm 0.2 | 8.4 \pm 0.2 | 10.8 \pm 0.2 | 17.7 \pm 0.4 |
| G5.89 (off) | < 0.5 | < 0.6 | < 0.7 | < 1.2 |
| G9.62 (on) | 3.2 \pm 0.2 | 3.5 \pm 0.2 | 4.4 \pm 0.2 | 7.3 \pm 0.4 |
| G9.62 (off) | 2.2 \pm 0.2 | 2.4 \pm 0.2 | 3.0 \pm 0.2 | 5.0 \pm 0.4 |
| G10.47 (on) | 9.5 \pm 0.3 | 10.2 \pm 0.3 | 13.1 \pm 0.4 | 21.4 \pm 0.6 |
| G10.47 (off) | 1.6 \pm 0.2 | 1.7 \pm 0.2 | 2.2 \pm 0.3 | 3.6 \pm 0.4 |
| G12.21 (on) | 2.1 \pm 0.2 | 2.3 \pm 0.2 | 2.9 \pm 0.3 | 4.8 \pm 0.5 |
| G12.21 (off) | < 0.7 | < 0.8 | < 1.0 | < 1.7 |
| G29.96 (on) | 3.5 \pm 0.2 | 3.8 \pm 0.2 | 4.9 \pm 0.2 | 7.9 \pm 0.3 |
| G29.96 (off) | < 0.5 | < 0.5 | < 0.6 | < 1.1 |
| G31.41 (on) | 4.8 \pm 0.3 | 5.2 \pm 0.3 | 6.6 \pm 0.4 | 10.8 \pm 0.6 |
| G31.41 (off) | < 0.6 | < 0.6 | < 0.8 | < 1.3 |
| G34.26 (on) | 9.8 \pm 0.2 | 10.5 \pm 0.2 | 13.5 \pm 0.3 | 22.0 \pm 0.5 |
| G34.26 (off) | 3.2 \pm 0.3 | 3.4 \pm 0.4 | 4.3 \pm 0.5 | 7.1 \pm 0.8 |
| G45.47 (on) | < 0.6 | < 0.6 | < 0.8 | < 1.3 |
| G45.47 (off) | < 0.8 | < 0.8 | < 1.1 | < 1.7 |
| G75.78 (on) | 2.7 \pm 0.2 | 2.9 \pm 0.2 | 3.7 \pm 0.3 | 6.1 \pm 0.4 |
| G75.78 (off) | < 0.6 | < 0.7 | < 0.9 | < 1.4 |

Firstly, it may simply reflect the fact that the DCN/HCN ratio was low when the molecules froze out. However, this is unlikely to be correct because to produce a gas-phase DCN/HCN ratio of order 10^{-3} requires temperatures larger than those of the OMC-1 ridge clouds, $\sim 50 - 70$ K, already quite large. Freeze-out of material at temperatures higher than 70 K is very inefficient. Note that the DCN/HCN fractionation reflects the fractionation in CH_2D^+ , a process which is efficient up to about 70 K and fairly insensitive to temperature below this value (Millar, Bennett & Herbst 1989). These authors find that the DCN/HCN ratio at early-time is $2.9 \pm 0.6 \cdot 10^{-3}$ over the temperature range of 30 - 70 K.

Secondly, a large DCN/HCN ratio in the gas phase prior to mantle formation could be diluted in the hot core gas through the preferential synthesis of HCN over DCN in the ice mantles. One could imagine a process by which, because of its lighter mass, H atoms could diffuse or quantum tunnel across the surface more efficiently than D atoms. This has the implication that the bulk of HCN is made on the grain - its fractional abundance must increase by an order of magnitude relative to DCN. Without a detailed quantum calculation of this system, it is impossible to confirm this. However, although H-atoms are more mobile on the surface, the D/H ratio on the surface is enhanced over cosmic values because it is enhanced in the gas phase and transfers this enhancement to grains upon collision. In addition, D atoms tend to be more strongly bound in molecules than H atoms, thus also favouring DCN formation over that of HCN. Enhancements, rather than dilution, of deuterium in molecules is certainly the expectation of simple models of grain chemistry (Tielens 1983, Brown & Millar 1989a,b, Charnley, Tielens & Rodgers 1997). A final argument against the view that HCN is formed pref-

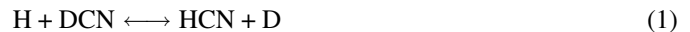
Table 5. HC^{15}N column densities and 3σ upper limits calculated for a range of excitation temperatures.

| Source | N(HC^{15}N) $\times 10^{12}$ cm $^{-2}$ | | | |
|--------------|---|----------------|----------------|----------------|
| | $T_x = 20$ | 30 | 50 | 100 K |
| G5.89 (on) | 9.7 \pm 0.4 | 9.6 \pm 0.4 | 11.4 \pm 0.5 | 17.8 \pm 0.8 |
| G5.89 (off) | < 1.2 | < 1.2 | < 1.5 | < 2.3 |
| G9.62 (on) | 4.2 \pm 0.3 | 4.2 \pm 0.3 | 5.0 \pm 0.4 | 7.8 \pm 0.6 |
| G9.62 (off) | < 1.1 | < 1.1 | < 1.3 | < 2.0 |
| G10.47 (on) | 5.0 \pm 1.0 | 4.9 \pm 0.9 | 5.9 \pm 1.1 | 9.2 \pm 1.8 |
| G10.47 (off) | < 1.1 | < 1.1 | < 1.3 | < 2.1 |
| G12.21 (on) | < 1.1 | < 1.0 | < 1.2 | < 1.9 |
| G12.21 (off) | < 1.4 | < 1.4 | < 1.7 | < 2.6 |
| G29.96 (on) | 3.7 \pm 0.4 | 3.7 \pm 0.4 | 4.4 \pm 0.4 | 6.9 \pm 0.7 |
| G29.96 (off) | < 1.4 | < 1.3 | < 1.6 | < 2.5 |
| G31.41 (on) | 6.6 \pm 0.7 | 6.5 \pm 0.6 | 7.8 \pm 0.8 | 12.1 \pm 1.2 |
| G31.41 (off) | < 1.3 | < 1.3 | < 1.6 | < 2.4 |
| G34.26 (on) | 18.7 \pm 1.2 | 18.5 \pm 1.2 | 22.1 \pm 1.4 | 34.4 \pm 2.2 |
| G34.26 (off) | < 1.9 | < 1.8 | < 2.2 | < 3.4 |
| G45.47 (on) | < 1.1 | < 1.1 | < 1.3 | < 2.0 |
| G45.47 (off) | < 1.0 | < 1.0 | < 1.2 | < 1.9 |
| G75.78 (on) | < 1.0 | < 1.0 | < 1.2 | < 1.9 |
| G75.78 (off) | < 1.9 | < 1.9 | < 2.3 | < 3.5 |

erentially on the dust is that the fractional abundance, using $^{14}\text{N}/^{15}\text{N} = 400$, lies between $10^{-9} - 10^{-8}$, entirely consistent with its abundance measured in molecular clouds, where the gas phase formation dominates.

Finally, the DCN/HCN ratio may reflect the conditions in the hot gas. Rodgers & Millar (1996) showed that, in general, the deuterium fractionation in evaporated parent molecules remains constant for up to 10^4 yrs. This is a consequence of the fact that most parent species have significant activation energy barriers for reactions with atomic H, so they can only be destroyed by ion-molecule chemistry, which is a slow process since the fractional ionisation is low. However, Charnley (1997) found that H_2S has a small activation energy for destruction by H atoms, and showed how the abundances of sulphur bearing species can be used to estimate the time since the grain mantles were evaporated. If, like H_2S , HCN and DCN are also able to react rapidly with atomic H and D, this provides a mechanism to alter the DCN/HCN ratio on this time scale.

Schilke et al. (1992) proposed that the reaction



can cycle deuterium between atomic D and the DCN molecule. They estimated a rate coefficient of 10^{-10} cm 3 s $^{-1}$, and an activation energy barrier of 200 K. Rodgers & Millar (1996) showed that this can alter the DCN/HCN ratios on a time scale of the order 100 yrs. However, Talbi, Ellinger & Herbst (1996) have performed quantum mechanical calculations on the HCNH system, and derived rate coefficients for the $\text{HNC} + \text{H} \leftrightarrow \text{HCN} + \text{H}$ isomerisation reaction. They found that the entrance channels on the left and right have activation energy barriers of 2100 K and

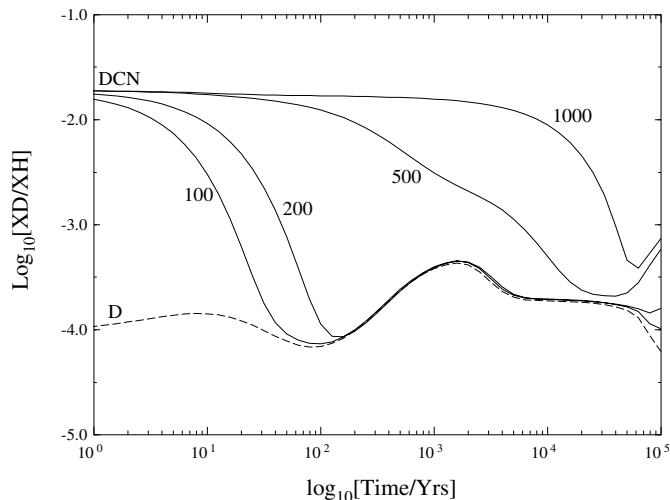


Fig. 3. DCN/HCN and D/H ratios as a function of time, following the evaporation of a deuterium rich ice at time $t = 0$. The four curves for DCN are labelled with the activation energy E_a (in Kelvin) assumed for the deuterium exchange reaction (1). The timescale is dependent on the hot core temperature assumed, reducing as the temperature increases; here, $T_k = 100$ K. For $T_k = 200$ K, the activation energies double, i.e. the reaction with activation energy $E_a = 200$ K at $T_k = 200$ K has the same timescale as $E_a = 100$ K, $T_k = 100$ K.

8900 K respectively. If the barriers in reaction (1) are similar, then it will take much longer than 100 yrs to alter the DCN/HCN ratio.

In order to investigate the evolution of the DCN/HCN ratio, we have modelled the DCN chemistry following its evaporation from grains. We assume that the initial DCN/HCN ratio is equal to the value of 0.02 observed in cold clouds, the initial fraction of hydrogen in atomic form is 10^{-5} , and the initial D/H ratio is 10^{-6} . The D/H ratios in other parent species are in the range 10^{-3} – 10^{-2} . Fig. 3 shows the DCN/HCN and D/H ratios as a function of time, for various values of the activation energy of reaction (1), assuming the hot core has a kinetic temperature of 100 K. We note that higher core temperatures reduce the timescale for DCN destruction, and temperatures of $T_k > 200$ K have been measured in the centres of some cores. However, on average the gas traced by our 21'' beam is cooler than 100 K (A.G. Gibb measured $T_x = 55$ K in G34.26, HC¹⁵N), so the true time taken to reduce the DCN/HCN abundance ratio to that observed is probably longer for each activation energy than we have shown. Hatchell et al. (1998) found that the hot cores for which we have calculated the DCN/HCN abundance ratio have ages less than 10^4 yrs, based on an analysis of sulphur chemistry (Charnley 1997). It can be seen that in order for the DCN/HCN ratio to be reduced to the values we observe on a time scale of $< 10^4$ yrs, the activation energy must be < 500 K.

4. Summary

Our observations do not answer definitively the question as to whether all of the DCN emission detected ‘on-core’ arises from

hot gas. Certainly the detection of DCN at the ‘off-core’ positions indicates that it is present in the halo gas. Hatchell et al. (1998) found that for 8 of the 9 sources observed here, the ‘on-core’ positions were line-rich and the ‘off-core’ positions were line-poor, indicating a core-halo structure.

However, following the arguments above, one can deduce that: (i) the low fractionation in HCN observed ‘on-core’ in these sources does not result from the accretion of material which already possesses the fractionation since relatively high temperatures are necessary to ensure that the DCN/HCN ratio is as low as 10^{-3} . At these temperatures mantle formation is not efficient due to thermal desorption; (ii) dilution of the DCN/HCN ratio from an initially large value by preferential formation of HCN on interstellar grains is not feasible since the fractional abundance of HCN in these hot cores is very similar to that observed in both warm and cold molecular clouds, indicating that the DCN/HCN ratio in molecular ices will reflect that in the condensing gas. Furthermore there is strong evidence from other molecules, including NH₂D (Brown & Millar 1989a), HDCO and D₂CO (Turner 1990, Brown & Millar 1989b), and CH₂DOH and CH₃OD (Charnley, Tielens & Rodgers 1997), that surface chemistry enhances rather than dilutes fractionation; (iii) the DCN/HCN ratio is altered in hot, post-evaporation gas by reaction with H atoms. These reactions can alter the DCN/HCN ratio in the hot gas on a timescale of $< 10,000$ years for an activation energy of < 500 K.

Acknowledgements. We would like to thank Iain Coulson at the JCMT for making some of the observations for us, and to Andy Gibb for information on G34.26. We are grateful to PATT for travel funds. Astrophysics at UMIST is supported by a grant from PPARC.

References

- Blake G. A., Sutton E. C., Masson C. R., Phillips T. R., 1987, ApJ, 315, 621
- Brown P. D., Millar T. J., 1989a, MNRAS 237, 661.
- Brown P. D., Millar T. J., 1989b, MNRAS 240, 25P.
- Brown R. D., Rice E. H. N., 1986, MNRAS 223, 429
- Caselli P., Hasegawa T. I., Herbst E., 1993, ApJ 408, 548.
- Charnley S. B., 1997, ApJ 481, 396.
- Charnley S. B., Tielens A. G. G. M., Millar T. J., 1992, ApJ 399, L71.
- Charnley S. B., Tielens A. G. G. M., Rodgers S. D., 1997, ApJ 482, L203.
- Dahmen G., Wilson T. L., Matteucci F., 1995, A&A 295, 194
- Hatchell J., Thompson M. A., Millar T. J., Macdonald G. H., 1998, A&A, submitted.
- Howe D. A., Millar T. J., 1993, MNRAS 262, 868.
- Kuan Y. J., Mehringer D. M., Synder L. E., 1996, ApJ 459, 619.
- Macdonald G. H., Gibb A. G., Habing R. J., and Millar T. J., 1996, A&AS 119, 333.
- Mehring D. M., Synder L. E., 1996, ApJ 471, 897.
- Miao Y. T., Mehringer D. M., Kuan Y. J., Synder L. E., 1995, ApJ 445, L59.
- Miao Y. T., Synder L. E., 1997, ApJ 480, L67.
- Millar T. J., Bennett A., Herbst E., 1989, ApJ 340, 906.
- Millar T. J., Macdonald G. H., Gibb A. G., 1997, A&A 325, 1163.
- Millar T. J., Macdonald G. H., Habing R. J., 1995, MNRAS 273, 25.

- Ohishi M., Ishikawa S., Yamamoto S., Saito S., Amano T., 1995, ApJ 446, L43.
- Rodgers S. D., Millar T. J., 1996, MNRAS 280, 1046.
- Schilke P., Walmsley C. M., Des Forêts G. P., Roueff E., Flower D. R., Guilloteau S., 1992, A&A 256, 595.
- Talbi D., Ellinger Y., and Herbst E., 1996, A&A 314, 688
- Tielens A. G. G. M., 1983, A&A 119, 177.
- Turner B. E., 1989, ApJ 347, L39.
- Turner B. E., 1990, ApJ 362, L29.
- Wooten A., 1987, In *Astrochemistry*, eds. M. S. Vardya and S. P. Tarafdar, Dordrecht, Reidel p. 311.